Since January 2020 Elsevier has created a COVID-19 resource centre with free information in English and Mandarin on the novel coronavirus COVID-19. The COVID-19 resource centre is hosted on Elsevier Connect, the company's public news and information website.

Microbial Pathogenesis 169 (2022) 105619

Contents lists available at ScienceDirect

Microbial Pathogenesis

journal homepage: www.elsevier.com/locate/micpath

The influence of new SARS-CoV-2 variant Omicron (B.1.1.529) on vaccine efficacy, its correlation to Delta variants: A computational approach

Prashant Ranjan [a], Neha [a], Chandra Devi [a], Kaaviyapriya Arulmozhi Devar [b], Parimal Das [a,*]

[a] Centre for Genetic Disorders, Institute of Science, Banaras Hindu University, Varanasi, Uttar Pradesh, India
[b] PSG College of Pharmacy, Coimbatore, Tamilnadu, India

ARTICLE INFO

Keywords:
Omicron
Delta variants
Immune evasion
In-silico analysis
MD Simulation

ABSTRACT

The newly discovered COVID variant B.1.1.529 in Botswana has more than 30 mutations in spike and many other in non-spike proteins, far more than any other SARS-CoV-2 variant accepted as a variant of concern by the WHO and officially named Omicron, and has sparked concern among scientists and the general public. Our findings provide insights into structural modification caused by the mutations in the Omicrons receptor-binding domain and look into the effects on interaction with the hosts neutralizing antibodies CR3022, B38, CB6, P2B–2F6, and REGN, as well as ACE2R using an *in silico* approach. Computational analysis revealed that the Omicron variant has a higher binding affinity for the human ACE2 receptor than the wild and Delta (AY.1 and AY.2 strains), but lower than the Delta AY.3 strain. MD simulation and docking analysis suggest that the omicron and Delta AY.3 were found to have relatively unstable RBD structures and hampered interactions with antibodies more than wild and Delta (AY.1 and AY.2), which may lead to relatively more pathogenicity and antibody escape. In addition, we observed lower binding affinity of Omicron for human monoclonal antibodies (CR3022, B38, CB6, and P2B2F6) when compared to wild and Delta (AY.1 & AY.2). However, the binding affinity of Omicron RBD variants for CR3022, B38, and P2B2F6 antibodies is lower as compared to Delta AY.3, which might promote immune evasion and reinfection and needs further experimental investigation.

1. Introduction

Viruses naturally have the ability to change their genetic makeup with time which doesn't affect it drastically but may affect host range, disease severity, transmissibility, diagnosis, re-infection, performance of vaccines and other therapeutics, etc. [1]. SARS-CoV-2 first reported in December 2019 in Wuhan, China, later became a pandemic [2]. Many variants have emerged since then, causing multiple waves of infection. Among those, Alpha (B.1.1.7 lineage), Beta (B.1.351), Gamma (P.1), and Delta (B.1.617.2) are categorised as variants of concern (VOCs) by WHO [3]. Several vaccines have been deployed for COVID-19 over time and data from different studies shows the effectiveness of vaccines against infection and the severity of the disease caused by the original SARS-CoV-2 strain. However, whether the vaccines are highly effective against other variants is still unknown and requires real-world validation [4].

The coronavirus spike (S) protein is important for interaction with the host cell. The S protein [1273aa] is composed of signal peptide (1–13aa), the S1 subunit (14–685aa), and the S2 subunit (686–1273aa). S1 and S2 mainly mediate host angiotensin-converting enzyme-2 (ACE2) receptor recognition and binding, followed by membrane fusion [5] [–] [8]. To be precise, it is the RBD domain (319–541aa residues) located in the S1 subunit that binds to the host cell ACE2 receptor [7]. Mutations in the spike region may affect the way the virus interacts with the host or responds to antibodies. The D614G mutation in spike protein enabled higher ACE2 binding affinity and was correlated with higher transmission and increased viral loads in COVID-19 patients [8–11]. The Delta variant of SARS-CoV-2 was the leading factor in the second wave [12]. Multiple sub-lineages of Delta variants were observed to be circulated among populations. From Nextstrain database, the PANGO lineage AY.1 contains T19R, T95I, G142D, E156-, F157-, R158G, W258L, K417 N, L452R, T478K, D614G, P681R, D950 N and PANGO AY.2 contains T19R, G142D, E156-, F157-, R158G, A222V, K417 N, L452R, T478K, D614G, P681R, D950 N and PANGO lineage AY.3

Abbreviations: H-bonding, hydrogen bonding; Rg, radius of gyration; RMSD, root mean square deviations; RMSF, root mean square fluctuations; SASA, Solvent Accessible Surface Area.

* Corresponding author. Centre for Genetic Disorders, Institute of Science, Banaras Hindu University, Varanasi 221005,Uttar Pradesh, India.
E-mail address: parimal@bhu.ac.in (P. Das).

https://doi.org/10.1016/j.micpath.2022.105619
Received 8 January 2022; Received in revised form 28 May 2022; Accepted 6 June 2022
Available online 8 June 2022

contains T19R, E156-, F157-, R158G, L452R, T478K, D614G, P681R, D950 N mutations in S protein. The K417 N, L452R, and T487K are common mutations in the AY.1 and AY.2 spike RBD, while the K417 N mutation is absent in the AY.3. D614G, P681R, and D950 N are other key S protein substitutions in the fusion region present in all Delta sub-lineages. The characteristic Delta variant mutation Del157-158 in the NTD of the S protein is considered to be associated with antibody escape [13,14]. The Delta variant showed higher replication rate, transmissibility, viral load as well as immune evasion [15] [–] [17]. The recently reported coronavirus variant B.1.1.529, named "Omicron" by WHO, is ringing the alarm around the world having 32 mutations in the spike protein that might help the virus escape immunity. From the GISAID database, these 32 conserved Spike mutations are A67V, Δ69–70, T95I, G142D/Δ143-145, Δ211/L212I, ins214EPE, G339D, S371L, S373P, S375F, K417 N, N440K, G446S, S477 N, T478K, E484A, Q493K, G496S, Q498R, N501Y, Y505H, T547K, D614G, H655Y, N679K, P681H, N764K, D796Y, N856K, Q954H, N969K, L981F. Besides these, the conserved non-Spike mutations are - NSP3–K38R, V1069I, Δ1265/L1266I, A1892T; NSP4–T492I; NSP5–P132H; NSP6–Δ105–107, A189V; NSP12–P323L; NSP14–I42V; E–T9I; M–D3G, Q19E, A63T; N–P13L, Δ31–33, R203K, G204R. Among these variations, N679K, P681H (adjacent to the furin cleavage site), N501Y (within receptor binding motif), D614G (Spike protein protomer) were earlier reported in other variants and found to be more transmissible and allow the virus to readily bind to the host cell ACE2R[8,18,19]. The mutation P681H has also been reported earlier in Alpha, Mu, some Gamma, and B.1.1.318 variants. According to WHO update on November 28, 2021, the current information about the transmissibility, disease severity, reinfection, effectiveness of existing vaccines, tests and treatment is not clear. Efforts are being made to better assess Omicron.

In this *in silico* study, we analysed the effect of mutations on the structure and binding affinity of the RBD region of Omicron and Delta variants (AY.1, AY.2, & AY.3) with ACE2R and with five different monoclonal SARS-CoV-2 neutralizing human antibodies, namely CR3022, B38, CB6, P2B–2F6, and REGN. The MD simulation done in this study provides insights into the structural variations. The docking analysis of the RBD region of Omicron and Delta variants (AY.1, AY.2, & AY.3) with the ACE2 receptor (ACE2R) and with selected antibodies showed differences in binding affinity when compared with the wild SARS-CoV-2 (original strain) spike-RBD region.

2. Methodology

2.1. Data sets

The crystal structure of different human neutralizing monoclonal antibodies CR3022 6W41 [20], B38 7BZ5[21], CB6 7C01[22], P2B–2F6 7BWJ [23], REGN 6XDG[24] and hACE2 receptor (PDB ID: 7A97) and S protein (7AD1) [25] were retrieved from PDB RCSB database.

2.2. Creation of mutant structure and preprocessing

The Swiss model was used to create the RBD mutants (Omicron, Delta AY.1, AY.2, and AY.3) [26]. 7AD1 was used as a template for homology modelling of mutations. A Modrefiner was employed to reduce the energy of the mutant structure [27]. PDB-Sum was used to evaluate the simulated structure [28]. The structure of the spike glycoprotein was preprocessed by eliminating all non-standard residues, including water molecules, and replacing them with hydrogen atoms using the Discovery studio programme [29]. The monomeric structure of the protein was examined for further research. By eliminating the spike glycoprotein chain from the complex and other nonstandard residues with the discovery studio, other antibodies-based complex structures were retrieved. The structure of the ACE2R was similarly constructed and preprocessed.

2.3. Prediction of physicochemical parameters, secondary structure and superimposition of structures

The Psipred online server [30] predicted the physicochemical characteristics, secondary structure and protein disorderness of Omicron, wild RBD and Delta variants. By using multialign, chimaera tool was used to superimpose wild and mutant RBD structures. The distance matrix of the wild and mutant structures was calculated by the superpose tool and used to visually discover substantial differences between the structures [31].

2.4. Docking analysis

The PatchDock server [32,33] was used to dock RBD mutant variants with ACE2R and distinct five monoclonal antibody structures, with an RMSD of 4.0 and complex type as default. The geometric form complementarity score was used to conduct the docking. A higher score suggests a stronger binding affinity. LigPlot plus v2.2 was used to view protein-protein and antibody-protein interactions [34]. The KABAT Scheme and the DIMPLOT script algorithm package integrated into LigPlot plus v2.2, were used to perform molecular interactions of antibodies and ACE2R with RBD variants.

2.5. Molecular simulation dynamics

GROMACS (GROMACS96 54a7 force field) [34] was used to investigate the molecular dynamics of wild-type and mutant RBD regions. MD simulation was used to produce time-dependent conformational alterations and protein modifications. To cope with dissolvable water surrounding protein, spc216.gro was utilised as a none-lite equilibrated 3 point dissolvable water model in a dodecahedron. The RBD wild type structure and mutations (Omicron, Delta AY.1, AY.2, & AY.3) were electrically neutralised by adding Na+59 and Cl-62, Na+68 and Cl-75, Na+76 and Cl-80 ions, and Na+90 and Cl-95 ions, respectively. The salt content was kept constant at 0.15 mol/L in all of the systems. Water molecules added to the wild RBD structure, Omicron, Delta AY.1 & AY.2, and Delta AY.3 were 20104, 23191, 23167, and 31118, respectively. At this phase, the protein was kept in the middle, at least 1.0 nm from the case edges. To minimise the energy, we adopted the steepest descent approach. The framework was then equilibrated at 300K temperature and 1atm for 100ps using the canonical ensemble (NVT) (constant number of particles, volume, and temperature) and the canonical ensemble (NPT) outfit (constant number of particles, pressure, and temperature). We extended the MD run time to 100ns after finishing the equilibrium measure. Gromacs tools (gmxrms, rmsf, gyrate hbond, sasa and gmx anaeig) were used to calculate root mean square deviation (RMSD), root mean square fluctuation (RMSF), gyrate for radius of gyration (Rg), H-bond (for intramolecular H-bonds), and solvent accessible surface area and Principal components analysis (PCA). The XMGRACE application was used to visualise the MD trajectory data [35].

3. Results

3.1. Physicochemical parameters, secondary structure and superimposition of structures

The superimposition of the RBD region of the wild and selected mutant variants suggests structural changes (Fig. 1). Secondary structure prediction analysis of Omicron has shown many changes in the helix, strands, and coils etc. as compared to wild (Fig. 2A and B). Also, the analysis suggests changes in S protein physiological properties like polarity and hydrophobicity at multiple positions (Fig. 2C and D). The RBD variants protein was determined to be intrinsically disordered as compared to wild (Fig. 3). Plaxco and Gross (2001) argue that protein disorder is critical to understanding protein function and folding mechanisms. A disordered protein that lacks a fixed or ordered three-

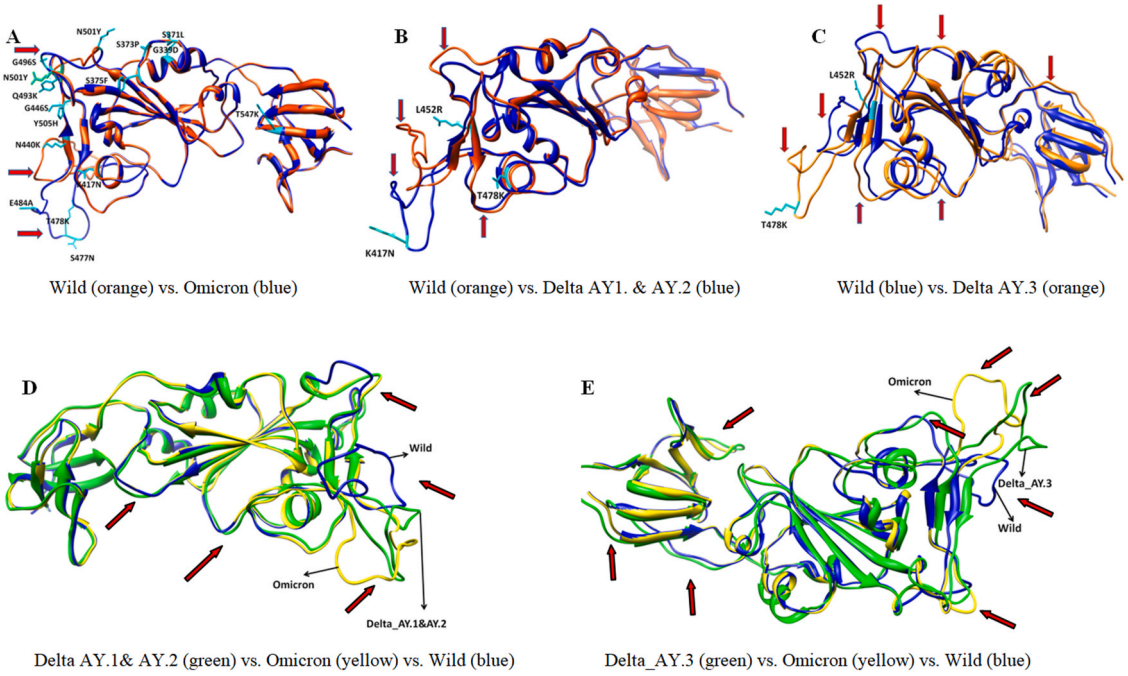

Fig. 1. Structural superimposition of wild and mutant variants of the RBD region of Spike. All of the variants have structural changes around the Antibody binding regions. A. Wild Vs Omicron B. Wild Vs Delta AY1. & AY.2 C. Wild Vs Delta AY.3 D. Delta AY.1 & AY.2 Vs Omicron Vs Wild. E. Delta AY.3 Vs Omicron Vs Wild. Red arrows indicate the structurally altered regions.

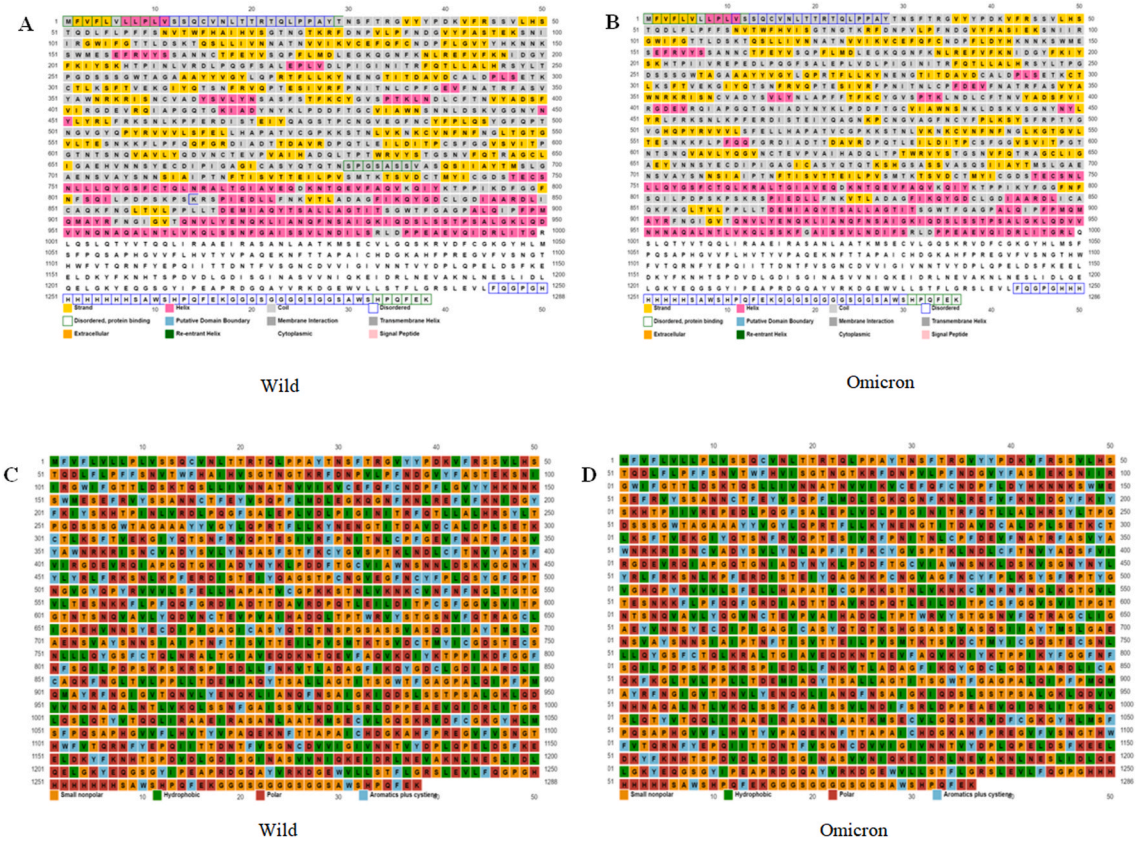

Fig. 2. Prediction of secondary structure and physiochemical parameter changes in the wild and Omicron. The polarity, non-polarity, and Hydrophobicity nature of Omicron showed changes as compared to wild.

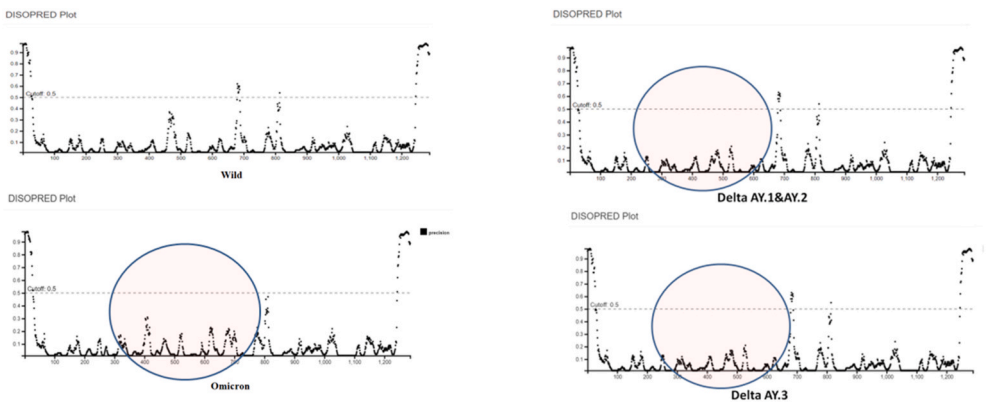

Fig. 3. Prediction of protein disorderness. The effect of the Protein disorders seen in the RBD regions of all variants (Omicron, Delta (AY.1 & AY.2 and Delta AY.3) as compared to Wild. The circle indicates the hampered regions.

dimensional structure and plays a diverse role in cell signaling and gene regulation.

Protein dysfunction has also been linked to disorders induced by protein mis-folding and aggregation in biology. Because intrinsically disordered proteins are involved in a variety of biological activities, it's not unexpected that some of them are linked to disease aetiology in humans. In fact, dysregulation and misfolding of ordinarily carefully regulated intrinsically disordered proteins can lead to their malfunction, which can lead to life-threatening pathological conditions. Mutations and/or environmental changes can impair a protein's ability to recognise appropriate binding partners, resulting in the creation of nonfunctional complexes and aggregates [36,37].

All these results suggest that mutations may have altered the structures and physiochemical properties of Omicron as compared to wild and the Delta variants. The difference distance matrix results show that Delta variant AY.3 had a significant change in the overall RBD structure

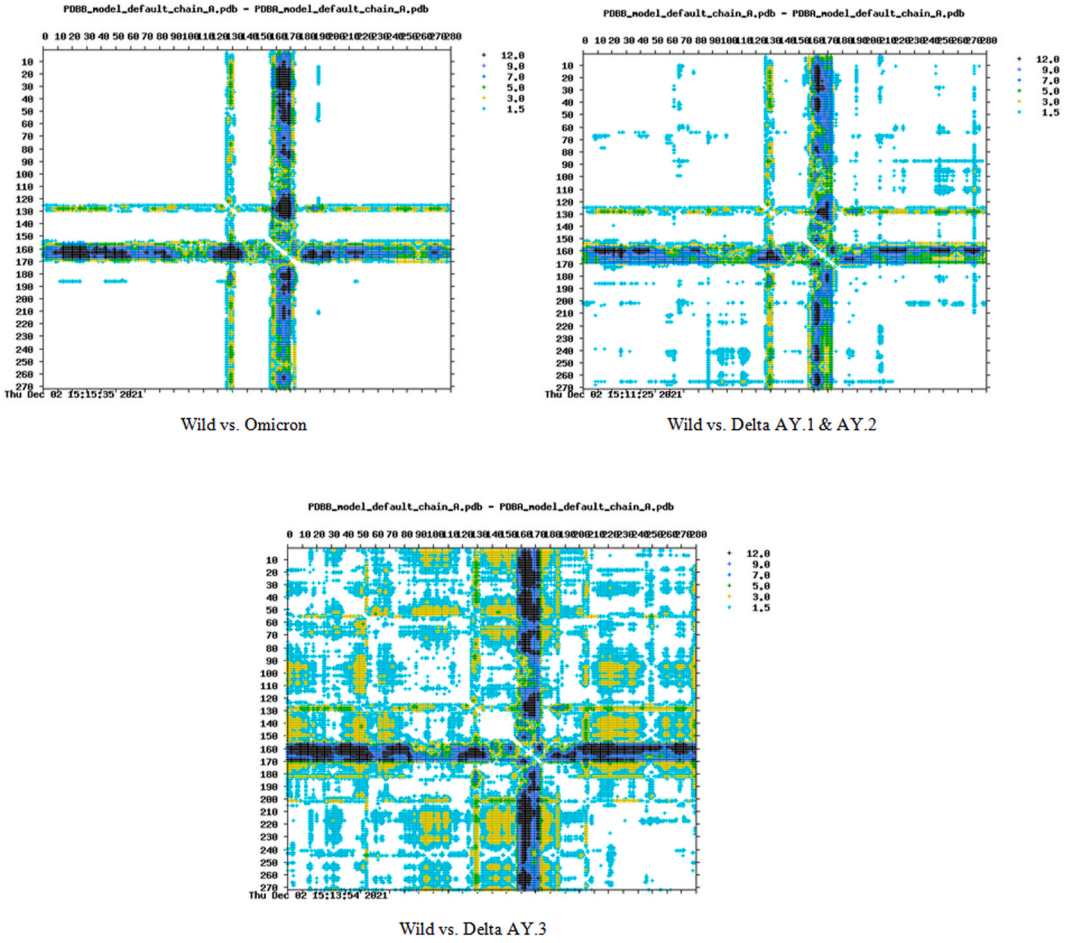

Fig. 4. Prediction of RBD variants' distance matrix (Wild, Omicron, Delta AY.1, AY.2 & AY.3).The lighter the region, the more similar the structures are. Likewise, the darker region corresponds to more prominent structures. The difference distance plot in Superpose shows six graded cutoffs. White depicts difference between 0 and 1.5 Å, yellow depicts difference between 1.5 and 3.0 Å, light green depicts difference between 3.0 and 5.0 Å, dark turquoise depicts difference between 5 and 7 Å, dark blue depicts difference between 7 and 9 Å, and black depicts difference between more than 9 Å.

when compared to Delta AY.1 & AY.2 and Omicron (Fig. 4).

3.2. Docking analysis

The docking analysis of the RBD region of Omicron and Delta variants (AY.1, AY.2, & AY.3) with ACE2R showed differences in binding affinity when compared with the wild SARS-CoV-2 spike-RBD region. The binding score determines the binding affinity. The binding score of ACE2R-Omicron RBD is higher (18208) than that of ACE2R-wild RBD, which is 17910, but it is less than ACE2R-Delta AY.3 (19084). The ACE2R-Delta AY.1 & 2 binding score 16886 is the lowest of all (Table 1). Through docking, the binding of the RBD region of Omicron with five different antibodies, viz. CR3022, B38, CB6, P2B–2F6, and REGN, was analysed and compared with wild spike-RBD region and Delta variant sub-lineages. The binding scores are shown in Table 2, and the different interactions are depicted in the supplementary file. The binding scores of antibodies CR3022, B38, CB6, P2B–2F6, and REGN with wild-RBD are 9248, 19152, 15984, 12776, and 14478, respectively. The binding score of antibodies CR3022, B38, CB6, P2B–2F6, and REGN with Omicron-RBD is 8768, 13240, 13660, 11900, and 14696, respectively, which is less than that of wild-RBD except REGN. Also, besides REGN, the binding score of the other four antibodies to Omicron-RBD is less than that of antibodies to Delta AY.1 and 2. The binding scores for Omicron-RBD vs. CR3022 (8768), Omicron-RBD vs. B38 (13240) and Omicron-RBD vs. P2B–2F6 (11900) are less than those of Delta AY. 3 (i.e., with CR3022 = 9158, B38 = 14308, and P2B–2F6 = 12124). The remaining two antibodies, CB6 and REGN, have a binding score slightly higher for Omicron-RBD (13660 and 14696) as compared to Delta AY. 3 (13206 and 13236).

3.3. Molecular simulations dynamics

The RMSD values of wild-type and mutant proteins were compared to better understand the impact of mutations on protein structure. We calculated the RMSD for all proteins' C alpha with reference to their original structures. The RBD structures of Omicron and Delta AY.3 fluctuate more than wild and Delta AY.1 & AY.2 according to RMSD plot (Fig. 5). Wild, Omicron, Delta (AY.1 & AY.2), and Delta AY.3 had average RMSD values of 0.25 nm, 0.39 nm, 0.26 nm, and 0.43 nm, respectively. We analysed atom's RMSF variations to examine how the mutation changed the dynamic behavior of the protein. Wild, Omicron, Delta (AY.1 & AY.2), and Delta AY.3 had average RMSF values of 0.164 nm, 0.201 nm, 0.157 nm, and 0.161 nm, respectively. Plots represent more fluctuations in RMSF of Omicron than Delta variants (Fig. 5). Rg fluctuation was greater in Omicron and Delta (AY.1 & AY.2), than wild while Delta AY.3 showed least changes (Fig. 5). Wild, Omicron, Delta (AY.1 & AY.2), and Delta AY.3 have average Rg values of 2.28 nm, 2.37 nm, 2.35 nm, and 2.26 nm, respectively. Wild, Omicron, Delta (AY.1 & AY.2), and Delta AY.3 have intramolecular h-bonding of 179.66, 172.50, 177.72, and 178.23, respectively. More fluctuation of intramolecular hydrogen bonding was observed in Omicron than other variants as compared to wild (Fig. 5). 156.47nm2, 152.75nm2, 152.01 nm2, and 152.34nm2 were the SASA values in Wild, Omicron, Delta (AY.1 & AY.2), and Delta AY.3 correspondingly (Fig. 5). The higher fluctuations were observed in Omicron amd Delta AY.3 as compared to wild and Delta AY.1&2.

Principal component analysis was carried out to investigate the major motions in the structure of RBD variants (Omicron, Delta, AY.1, AY.2, and AY.3) as compared to wild RBD. Fig. 6 shows the plot of the structural variance explained by the first 20 eigenvalues principal components (PCs). Fig. 6 A-D shows the 2D projection of the MD trajectory onto the PCs obtained by diagonalizing the covariance matrix of the atomic fluctuations. The clusters were compared to the dynamic behaviours of wild type and mutants, and the results indicated that clusters in wild type structures are clearly defined, covering the minimum region, whereas the Delta AY.3 and Omicron mutants occupied maximum regions. However, compared to Delta AY.3 and Omicron, Delta AY.1 and AY.2 covered smaller territories (Fig. 6A–D).

4. Discussion

Genetic lineages of SARS-CoV-2 have been arising and spreading around the world since the commencement of the COVID-19 pandemic. As per the WHO report and its international networks of experts till now a number of mutations in genomes of SARS-CoV-2 virions have been reported that are expected to be either neutral or moderately detrimental. Some mutations are expected to impact virus biology by affecting viral antigenicity, transmissibility, pathogenicity, and infectivity. Mutations in the spike protein of SARS-CoV-2 are expected to alter the antigenic phenotype of SARS-CoV-2 and affect immune recognition too that requires immediate attention [38]. The UK variant of B.1.1.7 lineage has 8 mutations in S protein that seems to be remaining susceptible for RNA-based COVID-19 vaccine BNT162b2 [39]. South African variants of lineage B.1.351 having E484K mutations reported being incompliant for neutralizing antibody and convalescent plasma and sera from the vaccinated population [40]. A variant of B.1.1.28 lineage first identified in Brazil has 10 RBD mutations and one within the furin cleavage site. This variant was also found to have resistance for RBD targeted neutralizing antibodies similar to B.1.351 [41,42]. Lineage B.1.526 contains E484K variation has been reported in New York first found to have resistance for therapeutic monoclonal antibodies meanwhile low susceptibility for neutralization by vaccine sera or convalescent plasma [43]. In 2021 B.1.67 (L452R & E484Q) RBD variant reported in India brought a deadlier second wave in the country within a short time. *In silico* analysis of structural stability and molecular simulation data of double mutant predicted reduced binding affinity for CR3022 antibody and lower vaccine efficacy of B.1.617.1 with antibody in comparison to wild type [34]. The Delta variant has become a more transmissible and dominant strain and the structural changes due to mutation may have caused the reduced response to vaccines. A study has shown that the mutation in the Delta variant causes reduced binding with neutralizing antibodies and thereby escaping the immunity [44].

The Omicron variant has been found to have the highest number of variations among all earlier reported SARS-CoV-2 variants which invoke an evaluation of the potential of infectivity and contagious characteristics of this variant as well as vaccine and antibody efficacy. Here we performed computational analysis of the changed structure of spike glycoprotein of Omicron variant and also compared with most transmissible and dominant Delta variants (AY.1, AY.2, & AY.3) and wild SARS-CoV-2 to investigate the discrepancy in susceptibility to the infection and potential for immune evasion. To estimate the binding efficiency of the variant's RBD region to ACE2R we carried out docking analysis of the RBD region to ACE2R. The binding score of ACE2R-Omicron RBD is 18208, ACE2R-wild RBD is 17910, ACE2R-Delta AY.3 is 19084 and ACE2R-Delta AY.1 & 2 are 16886 which shows that the omicron's RBD has higher binding affinity for ACE2R compared to wild type and Delta AY.1 & 2 whereas lower affinity compared to Delta AY.3 strain. The binding affinity of Delta AY.1 & 2 for ACE2R is least among

Table 1
The binding score from docking of RBD region of wild type, Omicron and Delta variants (AY.1, AY.2, & AY.3) with ACE2R.

Receptor	Binding score of Spike-wild RBD	Binding score of Omicron	Binding affinity	Binding score of Delta AY.1 & 2	Binding affinity	Binding score of Delta AY.3	Binding affinity
ACE2R	17910	18208	Higher	16886	Lesser	19084	Higher

Table 2
The binding score from docking of RBD region of wild type, Omicron and Delta variants (AY.1, AY.2, & AY.3) with CR3022, B38, CB6, P2B–2F6, and REGN antibodies.

Antibodies	Binding score of Spike-wild RBD	Binding score of Omicron	Binding affinity	Binding score of Delta AY.1 & AY.2	Binding affinity	Binding score of Delta AY.3	Binding affinity
CR3022	9248	8768	Lesser	8878	Lesser	9158	Lesser
B38	19152	13240	Lesser	15646	Lesser	14308	Lesser
CB6	15984	13660	Lesser	14012	Lesser	13206	Lesser
P2B–2F6	12776	11900	Lesser	13016	Higher	12124	Lesser
REGN	14478	14696	Higher	14122	Lesser	13236	Lesser

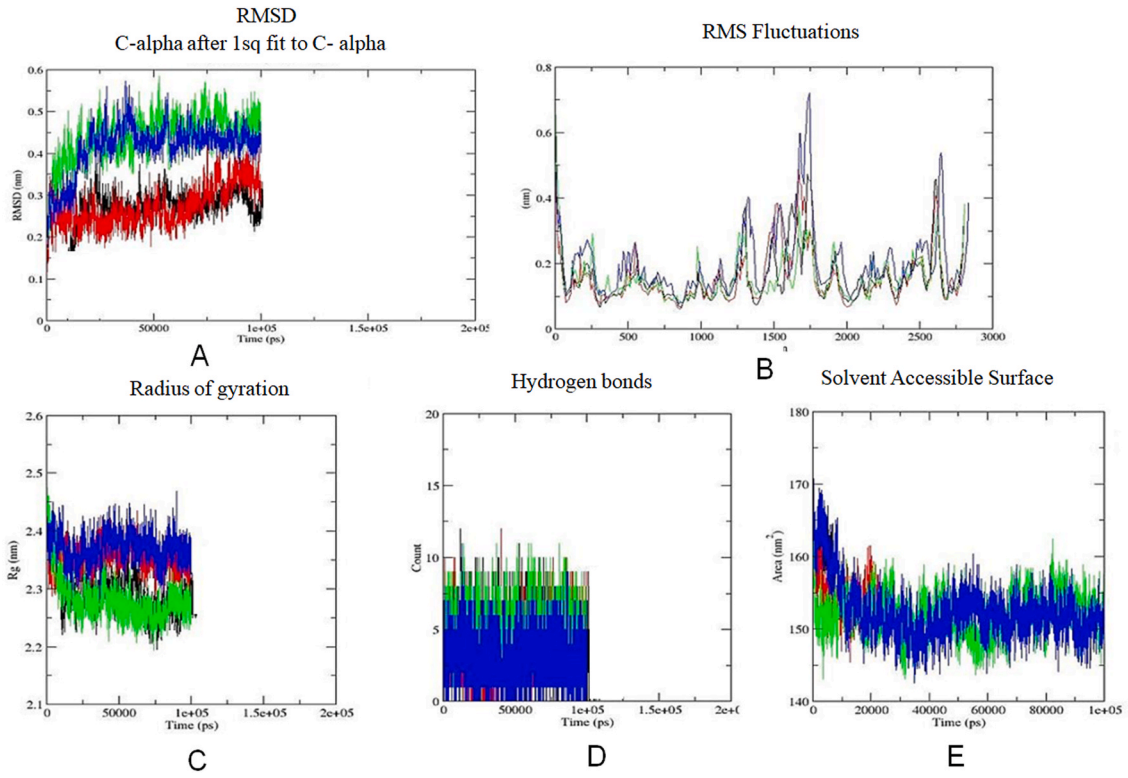

Fig. 5. Molecular simulation results of wild type and mutant variants (Omicron, Delta AY.1 & AY.2, and Delta AY.3). (A) RMSD plots, (B) RMSF plots, and (C) radius of gyration (Rg) plots, (D) Solvent accessible surface area (SASA), intramolecular H-bonds (E).Wild type-black, Omicron-blue, Delta AY.1 & AY.2- red, and Delta AY.3- green.

all. Docking for evaluating binding efficiency of the RBD region for five different human monoclonal antibodies viz. CR3022, B38, CB6, P2B–2F6, and REGN has also been done and found that the binding score of Omicron-RBD for antibodies CR3022, B38, CB6, P2B–2F6, and REGN is 8768, 13240, 13660, 11900, and 14696 respectively which is lesser than the binding score of wild-RBD and Delta AY.1 & 2 except for REGN. The binding score for Omicron-RBD for CR3022, B38, and P2B–2F6 is lesser than that of Delta AY.3 while for CB6 and REGN binding score is slightly higher for Omicron-RBD as compared to Delta AY.3. Our docking analysis revealed lower interaction of Omicrons-RBD with human antibodies compared to wild type and deadly Delta variant and higher interaction with ACE2R compared to wild type and Delta AY.1 & 2 while lower in comparison to Delta AY.3. Next, we superimposed the 3D structure of the RBD region of wild type with Omicron, Delta AY.1, AY.2 & AY.3 to predict alteration in structural and physiochemical parameters. This analysis shows intrinsically disordered Omicron-RBD protein along with a change in helix, strand, and the coil of Omicron structure as compared to the wild and Delta variant strains. Besides structural changes, polarity and hydrophobicity of Omicron were also found different from the wild type indicates that the omicron variant is structurally and physiochemicaly different from wild stain however major alterations in whole RBD structure were found in Delta AY.3 in contrast to Delta AY.1 & AY.2 and Omicron. MD simulations provide insights into protein's behavior in its natural environment and compute its trajectory over time, providing information on changed protein structure and fluctuations that may help to analyze flexibility and stability [45]. Pathological phenotypes can be caused by changes in protein stability and flexibility [46]. We evaluated the transient characteristics of wild-type and mutant Spike RBD to understand the functional and structural differences between the two. High fluctuations of RMSD were observed in Omicron and Delta AY.3 as compared with wild type while lower in Delta AY.1 & AY.2. After 20 ns wild, omicron and Delta (AY1,2 & 3) reached at equilibrium. The RMSD analysis showed lower average RMSD value of wild type in order [wild type (0.25 nm) < Delta (AY.1 & AY.2) (0.26 nm) < Omicron (0.39 nm) < Delta AY.3 (0.43 nm)] suggesting wild RBD was more stabilized and Delta AY.3 and Omicron

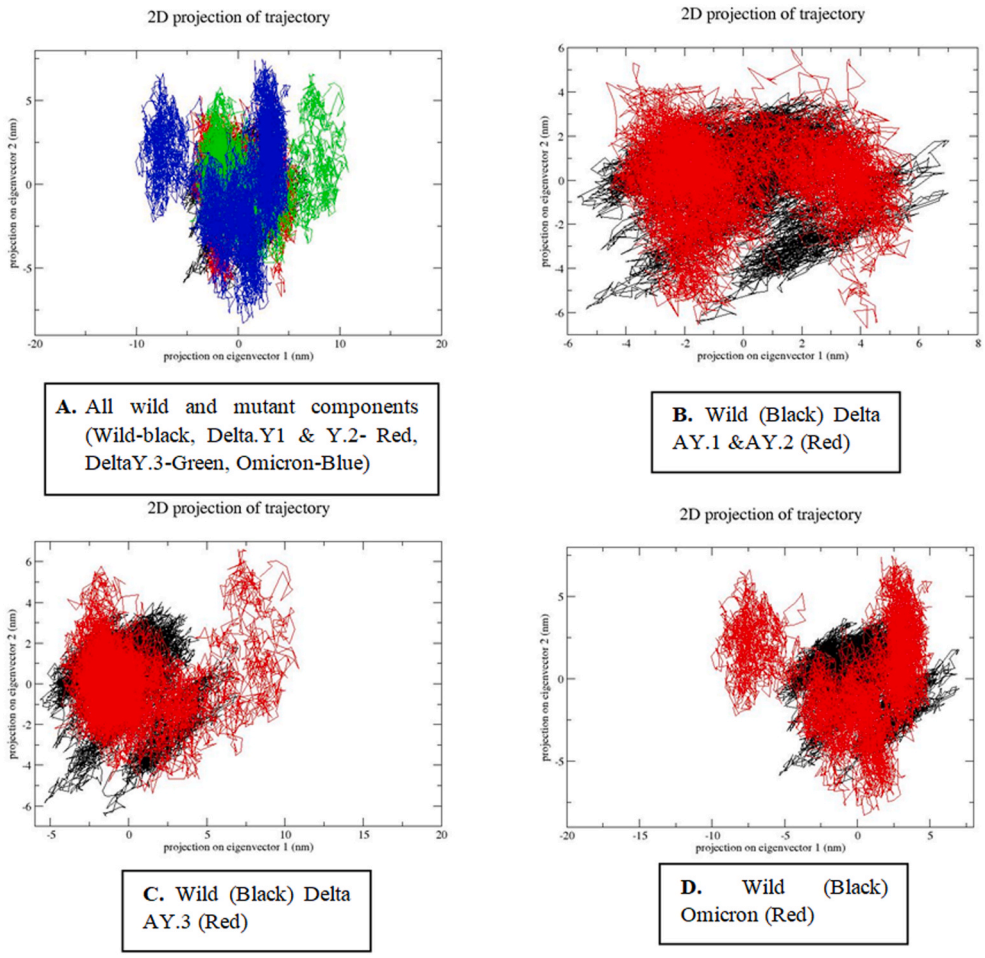

Fig. 6. Principal Component Analysis (PCA) of RBD structure of Delta and Omicron variants compared to the wild type. PCA of wild type and mutants spreads out across a vast region, showing distributed motion on the first two components, PC1, and PC2.

showed unstable structure. A higher RMSF value observed in Omicron and Delta Y.3 shows a more flexible structure than other variant which showed limited movement in the structure. In comparison to wild, the lowest Rg value is found in Delta AY.3 followed by Delta (AY.1 & 2) and Omicron that intimates more compactness in protein structure. However, Omicron and Delta AY.1 & 2 variants might be a less compact structure. Intramolecular H-bonds showed higher fluctuations in all mutant variants compared with wild type; albeit they overlapped at times and were higher and lower than wild type at other periods in the case of Delta (AY.1 & AY.2), Delta AY.3, and Omicron (Fig. 5). Intramolecular H-bonding showed that the wild type had a lower average number of H-bonds than Omicron, Delta (AY.1 & AY.2), and Delta AY.3 sequentially. However, very less hydrogen bonding observed in Omicron as compared to wild and other variants. The stiffness of proteins and their interactions may be affected by fluctuations in total intramolecular H-bonds [47]. There may be more interaction hampered in the case of Omicron because of fewer H-bonds observed. The highest SASA value was observed in the wild type than the variants in decreasing order: wild (156.47 nm^2) > Omicron (152.75 nm^2) Delta AY.3 (152.34 nm^2) >Delta (AY.1 & AY.3) (152.01 nm^2), which indicate that the examined variants are less accessible than the wild-type protein, which might affect their capacity to interact with other molecules. PCA showed that all mutant variants have structural differences as compared to wild-type. On the other hand, Delta AY.3 and Omicron structures, exhibit more variance than wild type, whereas Delta (AY.1 & 2) trajectories show a set of overlap. The conformational ensembles explored by Delta AY.3 and Omicron throughout simulation time differ from their wild-type counterparts.

5. Conclusion

In summary, this study anticipated more binding affinity of Omicron variant with ACE2R while lower affinity for neutralizing antibodies in contrast to wild type and Delta variant AY.1 & 2. However, Delta AY.3 shows highest binding affinity for ACE2R in contrast to the Omicron variant. In addition, the Delta AY.3 and Omicron variant is likely to be a relatively unstable that may lead to more pathogenicity as well as antibody escape than wild and Delta AY.1 & 2 strains. According to MD and docking analysis, Omicron and Delta variant AY.3 RBD region is majorly affected in comparison to Delta AY.1 & AY.2 and shows higher binding with ACE2R, unstable structure, hampered interactions with antibodies thus could still believed to be more pathogenic and immune evasive. Omicron had reduced binding affinity for CR3022, B38, CB6, and P2B2F6 than wild and Delta AY.1 and AY.2. However, as compared to Delta AY.3, the Omicron RBD region had a reduced binding affinity for CR3022, B38, and P2B2F6 antibodies, which might lead to antibody escape. The Delta variants (AY.1, AY.2, AY.3) have D614G, P681R, D950 N changes in the fusion region that binds to host receptor while Omicron has more changes (D614G, H655Y, N679K, P681H, N764K, D796Y, N856K, Q954H) in the fusion region. This may affect the host-pathogen interactions and ultimately transmissibility which need further validation from real-world data.

7. Conflicts of interest

The authors declare that they have no any conflict of interest.

Declaration of interests

☒ The authors declare that they have no known competing financial interests or personal relationships that could have appeared to influence the work reported in this paper.

☐ The authors declare the following financial interests/personal relationships which may be considered as potential competing interests.

CRediT authorship contribution statement

Prashant Ranjan: Writing – original draft, Software, Methodology, Formal analysis, Data curation, Conceptualization. **Neha:** Writing – original draft, Formal analysis, Data curation. **Chandra Devi:** Writing – original draft, Formal analysis, Data curation. **Kaaviyapriya Arulmozhi Devar:** Formal analysis. **Parimal Das:** Writing – review & editing, Supervision.

Data availability

Data will be made available on request.

6. Acknowledgements

Banaras Hindu University, Varanasi, India, supplied the internet and computer resources for this project.

Appendix A. Supplementary data

Supplementary data to this article can be found online at https://doi.org/10.1016/j.micpath.2022.105619.

References

[1] W.R. Fleischmann Jr., Viral Genetics, fourth ed., Med Microbiol, 1996.
[2] Y. Huang, M. Tu, S. Wang, S. Chen, W. Zhou, D. Chen, et al., Clinical characteristics of laboratory confirmed positive cases of SARS-CoV-2 infection in Wuhan, China: a retrospective single center analysis, Trav. Med. Infect. Dis. 36 (2020), 101606.
[3] F. Campbell, B. Archer, H. Laurenson-Schafer, Y. Jinnai, F. Konings, N. Batra, et al., Increased transmissibility and global spread of SARS-CoV-2 variants of concern as at June 2021, Euro Surveill. 26 (24) (2021), 2100509.
[4] J. Lopez Bernal, N. Andrews, C. Gower, E. Gallagher, R. Simmons, S. Thelwall, et al., Effectiveness of Covid-19 vaccines against the B. 1.617. 2 (Delta) variant, N. Engl. J. Med. (2021) 585–594.
[5] A.R. Fehr, S. Perlman, Coronaviruses: an overview of their replication and pathogenesis, Coronaviruses 1–23 (2015).
[6] M. Hoffmann, H. Kleine-Weber, S. Schroeder, N. Krüger, T. Herrler, S. Erichsen, et al., SARS-CoV-2 cell entry depends on ACE2 and TMPRSS2 and is blocked by a clinically proven protease inhibitor, Cell 181 (2) (2020) 271–280.
[7] Y. Huang, C. Yang, X. Xu, W. Xu, S. Liu, Structural and functional properties of SARS-CoV-2 spike protein: potential antivirus drug development for COVID-19, Acta Pharmacol. Sin. 41 (9) (2020) 1141–1149.
[8] L. Zhang, C.B. Jackson, H. Mou, A. Ojha, H. Peng, B.D. Quinlan, et al., SARS-CoV-2 spike-protein D614G mutation increases virion spike density and infectivity, Nat. Commun. 11 (1) (2020) 1–9.
[9] S. Ahamad, H. Kanipakam, D. Gupta, Insights into the structural and dynamical changes of spike glycoprotein mutations associated with SARS-CoV-2 host receptor binding, J. Biomol. Struct. Dyn. (2020) 1–13.
[10] P. Fuentes-Prior, Priming of SARS-CoV-2 S protein by several membrane-bound serine proteinases could explain enhanced viral infectivity and systemic COVID-19 infection, J. Biol. Chem. (2021) 296.
[11] B. Korber, W.M. Fischer, S. Gnanakaran, H. Yoon, J. Theiler, W. Abfalterer, et al., Tracking changes in SARS-CoV-2 Spike: evidence that D614G increases infectivity of the COVID-19 virus, Cell 182 (4) (2020) 812–827.
[12] L. Bian, Q. Gao, F. Gao, Q. Wang, Q. He, X. Wu, et al., Impact of the Delta variant on vaccine efficacy and response strategies, Expert Rev. Vaccines 20 (10) (2021) 1201–1209.
[13] A. Baj, F. Novazzi, F.D. Ferrante, A. Genoni, E. Tettamanzi, G. Catanoso, et al., Spike protein evolution in the SARS-CoV-2 Delta variant of concern: a case series from Northern Lombardy, Emerg. Microb. Infect. (2021) 1–10 (just-accepted).
[14] A. Chaudhari, D. Kumar, M. Joshi, A. Patel, E156/G and Arg158, Phe-157/del mutation in NTD of spike protein in B. 1.167. 2 lineage of SARS-CoV-2 leads to immune evasion through antibody escape, bioRxiv (2021).
[15] A. Bolze, E.T. Cirulli, S. Luo, S. White, T. Cassens, S. Jacobs, et al., Rapid displacement of SARS-CoV-2 variant B. 1.1. 7 by B. 1.617. 2 and P. 1 in the United States, bioRxiv (2021).
[16] B. Li, A. Deng, K. Li, Y. Hu, Z. Li, Q. Xiong, et al., Viral infection and transmission in a large well-traced outbreak caused by the Delta SARS-CoV-2 variant, medRxiv (2021).
[17] P. Mlcochova, S.A. Kemp, M.S. Dhar, G. Papa, B. Meng, I.A.T.M. Ferreira, et al., SARS-CoV-2 B. 1.617. 2 Delta variant replication and immune evasion, Nature (2021) 1–6.
[18] C. Scheepers, J. Everatt, D.G. Amoako, H. Tegally, C.K. Wibmer, A. Mnguni, et al., Emergence and phenotypic characterization of C. 1.2, a globally detected lineage that rapidly accumulated mutations of concern, medRxiv (2021) 2008–2021.
[19] K. Tao, P.L. Tzou, J. Nouhin, R.K. Gupta, T. de Oliveira, S.L. Kosakovsky Pond, et al., The biological and clinical significance of emerging SARS-CoV-2 variants, Nat. Rev. Genet. (2021) 1–17.
[20] M. Yuan, N.C. Wu, X. Zhu, C.-C.D. Lee, R.T.Y. So, H. Lv, et al., A highly conserved cryptic epitope in the receptor binding domains of SARS-CoV-2 and SARS-CoV, Science 368 (6491) (2020) 630–633, 80-.
[21] Y. Wu, F. Wang, C. Shen, W. Peng, D. Li, C. Zhao, et al., A noncompeting pair of human neutralizing antibodies block COVID-19 virus binding to its receptor ACE2, Science 368 (6496) (2020) 1274–1278, 80.
[22] R. Shi, C. Shan, X. Duan, Z. Chen, P. Liu, J. Song, et al., A human neutralizing antibody targets the receptor-binding site of SARS-CoV-2, Nature 584 (7819) (2020) 120–124.
[23] B. Ju, Q. Zhang, J. Ge, R. Wang, J. Sun, X. Ge, et al., Human neutralizing antibodies elicited by SARS-CoV-2 infection, Nature 584 (7819) (2020) 115–119.
[24] J. Hansen, A. Baum, K.E. Pascal, V. Russo, S. Giordano, E. Wloga, et al., Studies in humanized mice and convalescent humans yield a SARS-CoV-2 antibody cocktail, Science 369 (6506) (2020) 1010–1014, 80.
[25] S. Fatihi, S. Rathore, A. Pathak, D. Gahlot, M. Mukerji, N. Jatana, et al., A rigorous framework for detecting SARS-CoV-2 spike protein mutational ensemble from genomic and structural features, bioRxiv (2021).
[26] S. Lyskov, J.J. Gray, The RosettaDock server for local protein–protein docking, Nucleic Acids Res. 36 (suppl_2) (2008) W233–W238.
[27] D. Xu, Y. Zhang, Improving the physical realism and structural accuracy of protein models by a two-step atomic-level energy minimization, Biophys. J. 101 (10) (2011) 2525–2534.
[28] R.A. Laskowski, J. Jabłońska, L. Pravda, R.S. Vařeková, J.M. Thornton, PDBsum: structural summaries of PDB entries, Protein Sci. 27 (1) (2018) 129–134.
[29] D. Systèmes, Biovia, Discovery Studio Modeling Environment, Dassault Systèmes Biovia, San Diego, CA, USA, 2016.
[30] L.J. McGuffin, K. Bryson, D.T. Jones, The PSIPRED protein structure prediction server, Bioinformatics 16 (4) (2000) 404–405.
[31] R. Maiti, G.H. Van Domselaar, H. Zhang, D.S. Wishart, SuperPose: a simple server for sophisticated structural superposition, Nucleic Acids Res. 32 (suppl_2) (2004) W590–W594.
[32] P. Ranjan, P. Das, Understanding the impact of missense mutations on the structure and function of the EDA gene in X-linked hypohidrotic ectodermal dysplasia: a bioinformatics approach, J. Cell. Biochem. (2021).
[33] P. Ranjan, B. Mohapatra, P. Das, A Rational Drug Designing: what Bioinformatics Approach Tells about the Wisdom of Practicing Traditional Medicines for Screening the Potential of Ayurvedic and Natural Compounds for Their Inhibitory Effect against COVID-19 Spike, Indian strain Spike, Papa, 2020.
[34] P. Ranjan, Neha, C. Devi, P. Das, Bioinformatics analysis of SARS-CoV-2 RBD mutant variants and insights into antibody and ACE2 receptor binding [Internet], bioRxiv (2021 Jan 1), 2021.04.03.438113. Available from: http://biorxiv.org/content/early/2021/04/26/2021.04.03.438113.abstract.
[35] P.S. Srikumar, K. Rohini, P.K. Rajesh, Molecular dynamics simulations and principal component analysis on human laforin mutation W32G and W32G/K87A, Protein J. 33 (3) (2014) 289–295.
[36] S.H. Bates, W.H. Stearns, T.A. Dundon, M. Schubert, A.W.K. Tso, Y. Wang, et al., STAT3 signalling is required for leptin regulation of energy balance but not reproduction, Nature 421 (6925) (2003) 856–859.
[37] O. Schweers, E. Schönbrunn-Hanebeck, A. Marx, E. Mandelkow, Structural studies of tau protein and Alzheimer paired helical filaments show no evidence for beta-structure, J. Biol. Chem. 269 (39) (1994) 24290–24297.
[38] Q. Li, J. Wu, J. Nie, L. Zhang, H. Hao, S. Liu, et al., The impact of mutations in SARS-CoV-2 spike on viral infectivity and antigenicity, Cell 182 (5) (2020) 1284–1294.
[39] A. Muik, A.-K. Wallisch, B. Sänger, K.A. Swanson, J. Mühl, W. Chen, et al., Neutralization of SARS-CoV-2 lineage B. 1.1. 7 pseudovirus by BNT162b2 vaccine–elicited human sera, Science 371 (6534) (2021) 1152–1153, 80.
[40] P. Wang, M.S. Nair, L. Liu, S. Iketani, Y. Luo, Y. Guo, et al., Antibody resistance of SARS-CoV-2 variants B. 1.351 and B. 1.1. 7, Nature 593 (7857) (2021) 130–135.
[41] N.R. Faria, I.M. Claro, D. Candido, L.A.M. Franco, P.S. Andrade, T.M. Coletti, et al., Genomic characterisation of an emergent SARS-CoV-2 lineage in Manaus: preliminary findings, Virological 372 (2021) 815–821.
[42] W.T. Harvey, A.M. Carabelli, B. Jackson, R.K. Gupta, E.C. Thomson, E.M. Harrison, et al., SARS-CoV-2 variants, spike mutations and immune escape, Nat. Rev. Microbiol. 19 (7) (2021) 409–424.
[43] M.K. Annavajhala, H. Mohri, P. Wang, M. Nair, J.E. Zucker, Z. Sheng, et al., Emergence and expansion of the SARS-CoV-2 variant B. 1.526 identified in New York, medRxiv (2021) 2002–2021.
[44] P. Baral, N. Bhattarai, M.L. Hossen, V. Stebliankin, B.S. Gerstman, G. Narasimhan, et al., Mutation-induced changes in the receptor-binding interface of the SARS-CoV-2 Delta variant B. 1.617. 2 and implications for immune evasion, Biochem. Biophys. Res. Commun. 574 (2021) 14–19.

[45] B.B. Krebs, J.F. De Mesquita, Amyotrophic lateral sclerosis type 20-In Silico analysis and molecular dynamics simulation of hnRNPA1, PLoS One 11 (7) (2016), e0158939.

[46] F.I. Khan, D.-Q. Wei, K.-R. Gu, M.I. Hassan, S. Tabrez, Current updates on computer aided protein modeling and designing, Int. J. Biol. Macromol. 85 (2016) 48–62.

[47] R.E. Hubbard, M.K. Haider, Hydrogen Bonds in Proteins: Role and Strength, eLS, 2010.